

Orbital selective crossover and Mott transitions in an asymmetric Hubbard model of cold atoms in optical lattices

E. A. Winograd,¹ R. Chitra,² and M. J. Rozenberg^{1,3}

¹*Laboratoire de Physique des Solides, CNRS-UMR8502, Université de Paris-Sud, Orsay 91405, France.*

²*Laboratoire de Physique Theorique de la Matière Condensée, UMR 7600, Université de Pierre et Marie Curie, Jussieu, Paris-75005, France.*

³*Departamento de Física, FCEN, Universidad de Buenos Aires, Ciudad Universitaria Pab.I, (1428) Buenos Aires, Argentina.*

(Dated: October 13, 2018)

We study the asymmetric Hubbard model at half-filling as a generic model to describe the physics of two species of repulsively interacting fermionic cold atoms in optical lattices. We use Dynamical Mean Field Theory to obtain the paramagnetic phase diagram of the model as function of temperature, interaction strength and hopping asymmetry. A Mott transition with a region of two coexistent solutions is found for all nonzero values of the hopping asymmetry. At low temperatures the metallic phase is a heavy Fermi-liquid, qualitatively analogous to the Fermi liquid state of the symmetric Hubbard model. Above a coherence temperature, an orbital-selective crossover takes place, wherein one fermionic species effectively localizes, and the resulting bad metallic state resembles the non-Fermi liquid state of the Falicov-Kimball model. We compute observables relevant to cold atom systems such as the double occupation, the specific heat and entropy and characterize their behavior in the different phases.

PACS numbers: 67.85.Lm, 71.30.+h, 71.10.Fd

Quantum degenerate fermions can now be loaded onto optical lattices to recreate model hamiltonians with easily tunable physical parameters [1]. Two fermionic atomic species are minimally required to create a spin-1/2 model, where each type of atom is associated to a different projection of the spin. This can be achieved by either loading the optical lattice with atoms with two different hyperfine spin states or by two different atom species [1–5]. Remarkable aspects of the cold atom systems include the variety of lattice-types that can be realized, and the large range of interaction strengths that can be accessed, that may be up to several times the fermion bandwidth[6]. A lot of recent work has focused on the fermionic Hubbard model in 3D optical lattices, which is the paradigm of a strongly correlated fermionic system. For instance, a BCS-BEC crossover was observed in the attractive case using ^6Li atoms [7, 8], and also a Mott insulating state was reported in the repulsive case at half-filling using ^{40}K atoms[9, 10]. Although the exact realization of the Hubbard model may be achieved in cold atom systems, the generic situation, involving two different fermionic atomic species, will not exactly fulfill the requirement of spin symmetry. Thus, the model typically realized in an optical lattice would be an Asymmetric Hubbard model (AHM), which interpolates between the Hubbard model and the spinless Falicov-Kimball model (FKM), with or without population imbalance. This model, in the case of attractive interactions, has been considered in recent theoretical investigations that focused on the possibility of superconducting phases [2, 4]. The study of the AHM with repulsive interactions is therefore relevant and may provide needed guidance for current experimental investigations.

In this paper, we focus on the interesting case of the half filled AHM with no population imbalance and the associated paramagnetic Mott metal-insulator transition. For simplicity, we neglect the harmonic potential in our calculations, thus our results apply to the bulk of the optical lattice, away from the edges of the trap. We study the model within Dynamical Mean Field Theory (DMFT), a method which has significantly advanced our understanding of the Mott transition phenomenon [11, 12]. Here, we focus on paramagnetic states which may be realized in frustrated optical lattices. Our work shows that, akin to the Hubbard case, there is a region of coexistent solutions defined by two Mott-transitions at critical values U_{c1} and U_{c2} [11]. This region exists within the entire asymmetric regime, except right at the FKM end-point. While this observation may suggest that the AHM qualitatively behaves like the ordinary Hubbard model, we find that the actual situation is more subtle and cannot be described in terms of a simple interpolation between the two known limiting cases. In fact, in the metallic phase at low temperatures, we find a heavy-mass Fermi liquid state which is qualitatively similar to that of the spin-symmetric Hubbard model [11]. However, above a coherence temperature T_{coh} , instead of the standard incoherent metal seen in the Hubbard case, an orbital-selective crossover occurs, where the solution evolves to closely resemble the bad metallic state of the FKM. Thus, surprisingly, the behavior of the AHM embodies features of both, the Hubbard and the FKM. We also compute the double occupancy which is experimentally accessible [9], and the specific heat and entropy which are useful for the estimation of the temperature of experimental systems [10].

The Asymmetric Hubbard model Hamiltonian reads,

$$H = - \sum_{\langle ij \rangle; \sigma=\uparrow, \downarrow} t_{\sigma} c_{i\sigma}^{\dagger} c_{j\sigma} + U \sum_i (n_{i\uparrow} - 1/2)(n_{i\downarrow} - 1/2) \quad (1)$$

c, c^{\dagger} are the fermion creation and annihilation operators and the indices (i, j) and σ label the lattice sites and the two species of fermions, respectively. Defining $r \equiv t_{\downarrow}/t_{\uparrow}$, the AHM interpolates between the FKM at $r = 0$ (where one of the fermion species is immobile) and the spin-symmetric Hubbard model at $r = 1$. These two limits were studied extensively within the framework of DMFT (cf. see reviews of Refs. 11 and 12). We adopt a bounded semi-circular density of states for both fermionic bands with the half-bandwidths $D_{\sigma} = 2t_{\sigma}$. This choice presents a methodological advantage without affecting the qualitative physical behavior of the model [11]. The unit of energy, as customary, is set by $D_{\uparrow} = D = 1$. Within DMFT, the lattice model is map onto a quantum impurity problem subject to a self-consistency condition [11]. The self-consistency condition is given by,

$$\mathcal{G}_{0\sigma}^{-1}(i\omega_n) = i\omega_n + \mu_{\sigma} - t_{\sigma}^2 G_{\sigma}(i\omega_n) \quad (2)$$

where G_{σ} is the local Green's function of the fermions with spin σ and $\mathcal{G}_{0\sigma}$ are the bare Green's functions of the associated quantum impurity problem [11]. The impurity problem can be solved using exact diagonalization and quantum Monte Carlo techniques, whose implementation has been already detailed elsewhere [11].

The central quantities in the DMFT method are the local Green functions, $G_{\sigma}(\omega_n)$, where ω_n are the Matsubara frequencies. Here, since $t_{\uparrow} \neq t_{\downarrow}$ we should generically have $G_{\uparrow} \neq G_{\downarrow}$. Though the Matsubara Green's functions need to be analytically continued to the real frequency axis to obtain the spectral function (density of states), they nonetheless provide clear physical information. For instance, the density of states at the Fermi energy, which signals metallic or insulating states, is directly given by $-1/\pi \text{Im}[G_{\sigma}(\omega_n \rightarrow 0^+)]$.

At half-filling and $T = 0$ it is well known that the FKM has a Mott transition at a critical value $U_C^{FKM} = D$ whereas the HM is found to have two transitions at $U_{c1}^{HM} \approx 2.4D$ and $U_{c2}^{HM} \approx 3D$. The transition at U_{c1}^{HM} is related to the closing of the Mott gap, while that at U_{c2}^{HM} stems from the divergence of the carrier effective mass [11]. Both metallic and insulating solutions coexist in the region $U_{c1}^{HM} < U < U_{c2}^{HM}$. Given that both the Hubbard and FKM have metallic and Mott insulating phases, we expect a paramagnetic Mott metal-insulator transition in the AHM as a function of the repulsive interaction U for all r . Our results for the Green's functions at the generic value $r = 0.4$, for two values of the interaction $U = D$ and $3D$ are shown in the top left and right panels of Fig.1. The nonzero y-axis intercepts of both, G_{\uparrow} and G_{\downarrow} , in the data of the left top panel indicate the presence of (different) metallic states in the two

channels. On the other hand, as shown in the right top panel, at a higher value of the interaction U , the density of states vanishes, which signals an insulating state with the opening of a Mott gap for the up and down fermions. Moreover, as the gap is related to the slope of $G_{\sigma}(\omega_n)$ at low ω_n , we see that the gap has a similar magnitude for the two species. Though this establishes the existence of a Mott transition, we still need to understand how the Mott-transitions of the two end-cases (Hubbard and FKM) merge as a function of r and U .

We first analyze the metallic phase. In the standard Hubbard model ($r=1$), at low temperatures, one has a metallic Fermi liquid state with quasiparticles which have a renormalized mass m^* given by the self-energy Σ [13]. In such a Fermi liquid state, within DMFT, at low frequencies $\Sigma(\omega_n) \approx (1 - 1/Z)i\omega_n$, where Z is the quasiparticle residue [11]. Inputting the low frequency self energy into the definition of the Green's function, we obtain

$$G(\mathbf{k}, \omega_n) \approx \frac{1}{i\omega_n - \epsilon_{\mathbf{k}} - (1 - \frac{1}{Z})i\omega_n} = \frac{Z}{i\omega_n - Z\epsilon_{\mathbf{k}}}. \quad (3)$$

As (3) shows, the effective mass renormalization factor $m^* \propto 1/Z$, and at the Mott transition $Z \rightarrow 0$ and $m^* \rightarrow \infty$.

In the asymmetric model it is not a priori evident how the interactions will renormalize each one of the band masses. The results of the lower right panel of Fig.2 show the numerical results for Z_{σ} . We find that the mass renormalization of the two species is different, with the lighter one being more strongly suppressed by the effect of interactions. However, they both vanish at the same critical point. Thus, the ground-state of the system is an asymmetric Fermi liquid with two types of heavy quasiparticles, that beyond a critical value simultaneously localize into a Mott-Hubbard state.

As in the Hubbard case, the Fermi liquid state seen in the AHM exists below a certain coherence temperature T_{coh} and is characterized by a specific heat which is linear in temperature. Above T_{coh} , the thermal disorder is too strong for the quasiparticles to survive and the good metallic behavior is gradually lost. Our results for T_{coh} , obtained from the specific heat (to be discussed in detail later), are plotted in the lower left panel of Fig. 2. We find that this temperature is the same for both species consistent with the single Kondo temperature of the associated impurity problem[11]. As one increases the temperature above T_{coh} , the solution has a rapid crossover towards a new bad metallic state. Surprisingly, we find that this intermediate-temperature metallic state is not arbitrary, but essentially coincides with the non Fermi liquid solution of the FKM obtained at the same value of interaction U . The corresponding numerical result is shown in the lower right panel of Fig.1, where we compare the solution obtained at $T > T_{coh}$ with the FKM solution computed at the same value of T and U . We may interpret this rather striking result as if r effectively

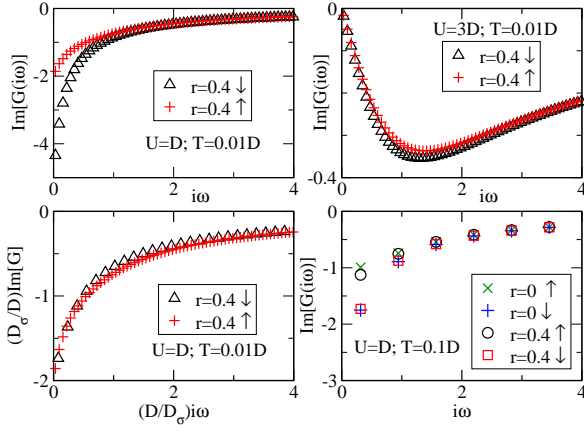


FIG. 1. (Color online) Matsubara Green's functions of the AHM for $r=0.4$ and $T=0.01D$. The top left panel shows a metallic solution for $U=D$ and the right one shows an insulating solution for $U=3D$. The lower left panel shows the pinning condition of the two metallic solutions ($\text{Im}[G_\sigma](\omega_n \rightarrow 0) = 2/D_\sigma$ at $T=0$) [11]. The lower right panel shows the same Green's functions at a higher temperature $T=0.1D > T_{coh}$. The solution essentially coincides with the FKM solution ($r=0$) computed at the same value of U .

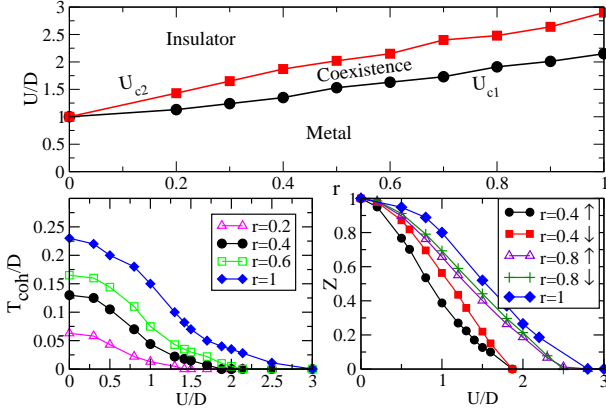


FIG. 2. (Color online) The top panel shows the $T=0$ phase diagram as function of r and U with the Mott transition boundaries U_{c1} and U_{c2} . The lower left (right) panel shows the behavior of T_{coh} (Z_σ) as a function of interaction U for various values of the asymmetry factor r . The size of the symbols are an estimate of the error bars.

renormalizes down to zero as $T \sim T_{coh}$. Since in the FKM one of the fermionic species is itinerant while the other is fully localized ($t_\downarrow=0$), the observed behavior in the AHM amounts to an orbital selective crossover to localization of the down spin fermions. The AHM can therefore be considered as a minimal model to realize an orbital selective transition, a concept that has recently received a lot of attention in the context of strongly correlated fermions in condensed matter systems [14, 15].

The $T=0$ phase diagram of the model as a function of asymmetry r and interaction U is shown in the top

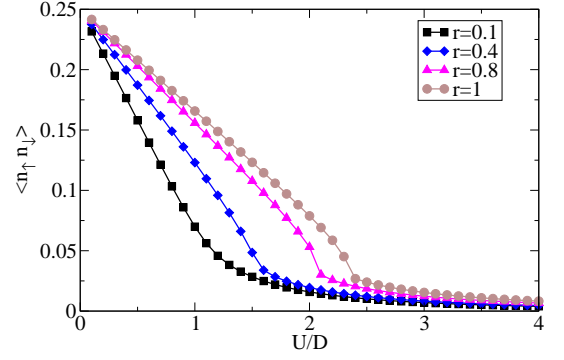


FIG. 3. (Color online) Double occupancy as function of U at $T=0.025D$, for different values of $r=t_\downarrow/t_\uparrow$. From top to bottom, the curves correspond to decreasing values of r .

panel of Fig.2. As discussed before, at low T , the AHM qualitatively behaves as the Hubbard model and has two critical Mott transition boundaries, U_{c1} and U_{c2} , that define a region of coexistent solutions [11]. The two critical lines merge at the FKM end-point. This coexistence survives for a small range of temperatures resulting in a first order metal-insulator transition line at low temperatures which culminates in a second order critical point [11]. The calculation of this small critical temperature is technically demanding and is left for future work. Similarly to the Hubbard case, we see in Fig.2 that for all $r \neq 0$, $Z \rightarrow 0$ as $U \rightarrow U_{c2}$ leading to a divergence of the effective mass at U_{c2} .

In order to establish a link between the behavior of the model and the physical observables accessible in cold atom systems on optical lattices, we compute the double occupation $\langle n_\uparrow n_\downarrow \rangle$, which can be used as a thermometer [16, 17]. In fact, this quantity is also closely related to an order parameter for the Mott metal-insulator transition [10, 18]. The results are shown in Fig.3 for various values of U and r at finite $T=0.025D$. At larger values of r there is a very sharp transition from the metal to the insulator state. The metal is characterized by linear decrease of the double occupation with increasing interaction U , while in the insulator, at larger values of the interaction, the double occupation remains low and weakly U -dependent. The rapid variation of $\langle n_\uparrow n_\downarrow \rangle$ with a sigmoidal shape between the two regimes is also an indication of the finite-temperature region of coexistent solutions that we discussed before [18]. At smaller values of r , when the system is more asymmetric, the double occupation rapidly decreases due to the very small coherence scale and the reduced values of the critical U . For the lower r values the temperature of the calculation is actually above T_{coh} (cf Fig.2), thus we observe a rather slow and wide crossover region for the evolution between the metal and the insulator.

Other experimentally relevant quantities we compute are the specific heat and the entropy which are required

to estimate the temperature of a cold atom system. In fact, these systems are in the sub-millikelvin regime and since they do not dissipate energy their evolution is considered to occur essentially along isentropic lines [19]. To understand the evolution of the specific heat and entropy, it is useful to start with the known cases of the Hubbard and FKM at $T=0$. In a regular Fermi liquid the entropy vanishes as $T \rightarrow 0$. However, there are also two other cases to be considered, which are unusual as they have unquenched entropy per site $S/N=\ln 2$ at $T=0$ (we set the Boltzmann constant $k_B=1$). One is the paramagnetic Mott-insulator, with one localized particle per site, which only has the two spin-states as remanent degree of freedom. The other case is the bad metallic state of the FKM, where the localized particles are disordered and have equal probability of occupying or not each of the N lattice sites, thus contributing the $\ln 2$ to the entropy at half-filling. The itinerant particles, in contrast, adjust to the potential created by the former and form a band that contributes no entropy at $T = 0$. Consequently, starting from the Fermi liquid state of the AHM, we expect strong variations of the specific heat for both, the transition to the Mott insulator and the crossover to the orbital-selective bad metallic state.

Our results for the specific heat and entropy are plotted in Fig.4. The left side panels of Fig.4 show the evolution of C_v in the metallic phase for different values of r . Note that for all $r \neq 0$ and low enough T and U , the system is a normal Fermi liquid with the specific heat $C_v = \gamma T$ and $S \propto T$ with γ proportional to the mean effective mass of the quasiparticles. As the temperature increases and reaches T_{coh} , the singlet Fermi-liquid metallic state breaks down and the system crosses over to the orbitally selected bad-metal, which has FKM-like behavior, thus having an entropy of $\ln 2$. This is clearly seen in the lower right panel of Fig.4, where after an initial linear increase, the entropy attains a small plateau around $\ln 2$. This plateau is concomitant with the first maximum observed in the $C_v(T)$ at a $T \sim T_{coh}$. Physically, it corresponds to the orbital selection, i.e., the effective localization of the heavy-particle band. As T is further increased, the remaining degrees of freedom will eventually contribute their $\ln 2$ to the entropy, producing a second maximum in C_v at the bare energy scale $T \sim t_{\uparrow}=D/2$. In the high- T limit the specific heat decreases and the entropy saturates to the maximal value $\ln 4$. For comparison, the behavior of the specific heat and the entropy of a typical Mott insulating state at higher interaction $U = 2D$ and $r = 0.4$ is also shown in the right panel of Fig.4. At low T , $C_v(T)$ shows activated behavior indicating the presence of the Mott gap. We also observe, consistent with our previous discussion, that the entropy starts from the unquenched value $\ln 2$, and reaches $\ln 4$ in the high- T limit.

To conclude, we have studied the behavior of the asymmetric Hubbard model as a generic model for two species of fermionic cold atoms loaded onto an optical lattice.

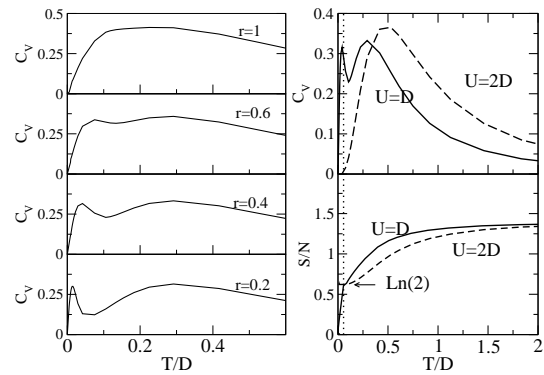


FIG. 4. Left panels: Specific heat as function of T for $U=D$ and different values of r . For $r=1$ the linear Fermi-liquid behavior is observed. As r decreases, a two-peak structure is visible. The first peak moves to lower T with decreasing r , revealing the reduction of T_{coh} and the increase of the effective mass (from the increase of the slope). Right panels: C_v (top) and entropy (bottom) as a function of T for $r=0.4$ and $U=D$ (metal) and $U=2D$ (Mott insulator).

We determined the phase diagram and found a Mott metal-insulator transition for all degrees of asymmetry. The Mott transition scenario is the same as that of the Hubbard model for all nonzero values of the asymmetry r . Within the metallic state, we found an interesting temperature-driven orbital selective crossover. At low temperatures the AHM has the same qualitative behavior as the *symmetric* Hubbard model, however with two different heavy mass Fermi-liquids. These two liquids have, nevertheless, a single coherence temperature. Above a coherence temperature, one fermionic species localizes and the system exhibits non-Fermi liquid behavior similar to that of the Falicov-Kimball model. We also computed the double occupation and some thermodynamical observables which may permit the experimental identification of this remarkable physical behavior.

E. A. W. is financially supported by the program ANR-09-RPDOC-019-01.

-
- [1] I. Bloch, J. Dalibard, and W. Zwerger, Rev. Mod. Phys. **80**, 885 (2008).
 - [2] M. A. Cazalilla, A. F. Ho, and T. Giamarchi, Phys. Rev. Lett. **95**, 226402 (2005).
 - [3] B. Wang, H.-D. Chen, and S. Das Sarma, Phys. Rev. A **79**, 051604 (2009).
 - [4] T.-L. Dao, A. Georges, and M. Capone, Phys. Rev. B **76**, 104517 (2007).
 - [5] G.-D. Lin, W. Yi, and L.-M. Duan, Phys. Rev. A **74**, 031604 (2006).
 - [6] T. Esslinger, arXiv:1007.0012 [cond-mat.quant-gas] (preprint).
 - [7] J. K. Chin, D. E. Miller, Y. Liu, C. Stan, W. Setiawan, C. Sanner, K. Xu, and W. Ketterle, Nature **443**, 961 (2006).

- [8] S. Giorgini, L. P. Pitaevskii, and S. Stringari, *Rev. Mod. Phys.* **80**, 1215 (2008).
- [9] R. Jördens, N. Strohmaier, K. Günter, H. Moritz, and T. Esslinger, *Nature* **455**, 204 (2008).
- [10] U. Schneider, L. Hackermüller, S. Will, T. Best, I. Bloch, T. A. Costi, R. W. Helmes, D. Rasch, and A. Rosch, *Science* **322**, 1520 (2008).
- [11] A. Georges, G. Kotliar, W. Krauth, and M. J. Rozenberg, *Rev. Mod. Phys.* **68**, 13 (1996).
- [12] J. K. Freericks and V. Zlatić, *Rev. Mod. Phys.* **75**, 1333 (2003).
- [13] G. D. Mahan, Many-Particle Physics (Plenum, New York, N.Y., 1993), 2nd ed.
- [14] M. Vojta, *Journal of Low Temperature Physics* **161**, 203 (2010).
- [15] S. Biermann, L. de' Medici, and A. Georges, *Phys. Rev. Lett.* **95**, 206401 (2005).
- [16] R. Jördens, L. Tarruell, D. Greif, T. Uehlinger, N. Strohmaier, H. Moritz, T. Esslinger, L. De Leo, C. Kollath, A. Georges, et al., *Phys. Rev. Lett.* **104**, 180401 (2010).
- [17] T. Stöferle, H. Moritz, K. Günter, M. Köhl, and T. Esslinger, *Phys. Rev. Lett.* **96**, 030401 (2006).
- [18] M. J. Rozenberg, R. Chitra, and G. Kotliar, *Phys. Rev. Lett.* **83**, 3498 (1999).
- [19] F. Werner, O. Parcollet, A. Georges, and S. R. Hassan, *Phys. Rev. Lett.* **95**, 056401 (2005).